Molecular Cancer Therapeutics

Inhibition of vascular endothelial growth factor reduces angiogenesis and modulates immune cell infiltration of orthotopic breast cancer xenografts

Christina L. Roland, Sean P. Dineen, Kristi D. Lynn, et al.

Mol Cancer Ther 2009;8:1761-1771. Published OnlineFirst June 30, 2009.

Updated version	Access the most recent version of this article at: doi:10.1158/1535-7163.MCT-09-0280

Cited Articles	This article cites by 49 articles, 21 of which you can access for free at: http://mct.aacrjournals.org/content/8/7/1761.full.html#ref-list-1
Citing articles	This article has been cited by 3 HighWire-hosted articles. Access the articles at: http://mct.aacrjournals.org/content/8/7/1761.full.html#related-urls

E-mail alerts	Sign up to receive free email-alerts related to this article or journal.
Reprints and Subscriptions	To order reprints of this article or to subscribe to the journal, contact the AACR Publications Department at pubs@aacr.org.
Permissions	To request permission to re-use all or part of this article, contact the AACR Publications Department at permissions@aacr.org.

Inhibition of vascular endothelial growth factor reduces angiogenesis and modulates immune cell infiltration of orthotopic breast cancer xenografts

Christina L. Roland,[1,2] Sean P. Dineen,[1,2] Kristi D. Lynn,[1,2] Laura A. Sullivan,[1,2] Michael T. Dellinger,[1,2] Leila Sadegh,[1,2] James P. Sullivan,[2] David S. Shames,[2,3] and Rolf A. Brekken[1,2,3]

[1]Division of Surgical Oncology, Department of Surgery; [2]Hamon Center for Therapeutic Oncology Research; and [3]Department of Pharmacology, University of Texas Southwestern Medical School, Dallas, Texas

Abstract

Vascular endothelial growth factor (VEGF) is a primary stimulant of angiogenesis and is a macrophage chemotactic protein. Inhibition of VEGF is beneficial in combination with chemotherapy for some breast cancer patients. However, the mechanism by which inhibition of VEGF affects tumor growth seems to involve more than its effect on endothelial cells. In general, increased immune cell infiltration into breast tumors confers a worse prognosis. We have shown previously that 2C3, a mouse monoclonal antibody that prevents VEGF from binding to VEGF receptor 2 (VEGFR2), decreases tumor growth, angiogenesis, and macrophage infiltration into pancreatic tumors and therefore hypothesized that r84, a fully human IgG that phenocopies 2C3, would similarly affect breast tumor growth and immune cell infiltration. In this study, we show that anti-VEGF therapy with bevacizumab, 2C3, or r84 inhibits the growth of established orthotopic MDA-MB-231 breast tumors in severe combined immunodeficiency (SCID) mice, reduces tumor microvessel density, limits the infiltration of tumor-associated macrophages, but is associated with elevated numbers of tumor-associated neutrophils. In addition, we found that treatment with r84 reduced the number of CD11b$^+$Gr1$^+$ double-positive cells in the tumor compared with tumors from control-treated animals. These results show that selective inhibition of VEGFR2 with an anti-VEGF antibody is sufficient for effective blockade of the protumorigenic activity of VEGF in breast cancer xenografts. These findings further define the complex molecular interactions in the tumor microenvironment and provide a translational tool that may be relevant to the treatment of breast cancer. [Mol Cancer Ther 2009;8(7):1761–71]

Note: C.L. Roland, S.P. Dineen, and K.D. Lynn have equal contributions.

Requests for reprints: Rolf A. Brekken, Hamon Center for Therapeutic Oncology Research, University of Texas Southwestern Medical Center, 6000 Harry Hines Boulevard, Dallas, TX 75390-8593. Phone: 214-648-5151; Fax: 214-648-4940. E-mail: rolf.brekken@utsouthwestern.edu

Introduction

Angiogenesis, the process by which the existing vascular network expands to form new blood vessels, is required for the growth of solid tumors (1). For this reason, tumor angiogenesis has become a critical target for cancer therapy. Vascular endothelial growth factor (VEGF), a primary stimulant of angiogenesis, binds and activates VEGF receptor 1 (VEGFR1) and VEGFR2 (2). Although the function of VEGFR2 in tumor angiogenesis has been characterized thoroughly, the function of VEGFR1 has not been well defined. However, there is evidence to support a function for VEGFR1 in tumor cell survival and invasion (3, 4). In addition, VEGFR1 has been shown to negatively regulate VEGFR2 activity (5, 6). Furthermore, expression of neuropilin-1 (Nrp-1) and Nrp-2, coreceptors for VEGF, is associated with poor prognosis in breast cancer (7), which might be due to coreceptor-mediated enhanced signaling through VEGFR2 (8).

Bevacizumab (Avastin, Genentech), a humanized monoclonal antibody that binds human VEGF and prevents activation of VEGFR1 and VEGFR2, was first successful in the clinic for the treatment of metastatic colon cancer in combination with chemotherapy in 2004 (9). Recently, bevacizumab has also been approved for the treatment of metastatic HER2/NEU–negative breast cancer (10). The clinical success of bevacizumab has bolstered the development and testing of agents that directly target VEGF, selectively inhibit VEGFR1 or VEGFR2, or promiscuously block both VEGF receptors as well as other receptor tyrosine kinases (11, 12).

2C3 is an anti-VEGF mouse monoclonal antibody that prevents human VEGF from binding to VEGFR2 but not VEGFR1 (13). r84 is a fully human IgG that has the same characteristics as 2C3 but also binds mouse and human VEGF.[4] Inhibition of VEGFR2 activity with 2C3 is an effective antiangiogenic therapy in preclinical orthotopic breast and pancreatic cancer models, wherein it significantly reduces tumor burden, tumor microvessel density, macrophage infiltration,

---

[4] L.A. Sullivan, et al., unpublished data.

and the number of metastatic events compared with an iso-type-matched control antibody (14–17). These studies illustrate that selective inhibition of VEGFR2 is sufficient for effective control of tumor growth in preclinical models. The antitumor effect of 2C3 is due in part to reduction of VEGF-induced angiogenesis. Immune cells also express receptors for VEGF; however, the effect of anti-VEGF therapy on the infiltration of immune cells into tumors has not been fully characterized.

Infiltrating inflammatory cells constitute a large component of the overall tumor mass (18, 19). Initially, this was thought to represent an attempt by the host to combat the tumor; however, it has been increasingly recognized that most tumors are not recognized as foreign and that the inflammatory/immune infiltrate promotes tumor growth and metastasis (18, 19). Most clinical studies indicate that increased macrophage infiltration into tumors confers a negative prognosis in breast cancer (20, 21). In animal studies, depletion of macrophages has led to decreased tumor growth in breast (22) and Ewing's sarcoma models (23). Recent studies indicate that selective reduction of macrophage infiltration in cervical cancer results in compensatory neutrophil infiltration into the tumor and subsequent angiogenic recovery (24). Previously, we and others have shown that anti-VEGF therapy lead to a reduction in macrophage infiltration in tumor xenograft models (14, 16, 25).

Aside from macrophages, it has also been reported that neutrophils can mediate the angiogenic switch in a transgenic model of pancreatic cancer (26). Furthermore, myeloid-derived suppressor cells ($CD11b^+Gr1^+$) are also an important contributor to tumor progression. In the tumor microenvironment, these cells secrete immunosuppressive mediators and induce T-lymphocyte dysfunction (27, 28). In addition, myeloid-derived suppressor cells can mediate tumor resistance to anti-VEGF therapy (29). Unlike other myeloid cell types, increased tumor-infiltrating dendritic cells is associated with improved prognosis, and, specifically, the number of $CD83^+$ tumor-infiltrating dendritic cells has been shown to inversely correlate with lymph node metastasis and tissue expression of VEGF and transforming growth factor β in human breast cancer specimens (30). In support of this, studies in non–tumor-bearing animals have shown that stimulation of VEGFR2 leads to increased myeloid-derived suppressor cells and decreased $CD86^+$ dendritic cells in the spleen and lymph nodes of mice after chronic VEGF treatment (31).

Based on these data, we hypothesized that r84, a fully human IgG that is functionally identical to 2C3, would reduce breast tumor growth and immune cell infiltration. In the present study, we investigate the antitumor effects of three anti-VEGF monoclonal antibodies, 2C3, r84, and bevacizumab, in an orthotopic model of breast cancer. We show that all three antibodies inhibit tumor growth, microvessel density, and macrophage infiltration. Furthermore, neutrophil infiltration was increased following treatment with each antibody. Interestingly, the number of $CD11b^+Gr1^+$ cells was reduced in tumors from mice treated with r84 but remained unchanged in tumors from 2C3- and bevacizumab-treated animals. Finally, there was an increase in the number of $CD83^+$ dendritic cells in tumors from r84-treated animals.

These findings show that r84 effectively controls the growth of human breast cancer xenografts and support the evaluation of r84 as an antiangiogenic agent in clinical studies.

Materials and Methods
Cell Lines and Culture Conditions
The human breast carcinoma cell line MDA-MB-231 was obtained from the American Type Culture Collection. Cells were maintained at 37°C in a mixture of 5% CO_2 and 95% air in DMEM (Invitrogen) supplemented with 10% FCS (Gemini Bio-Products).

Anti-VEGF Antibodies
Bevacizumab (Avastin, Genentech) was purchased from the clinical pharmacy at University of Texas Southwestern. 2C3, a mouse IgG2a, was produced in our laboratory, as described (13). The production and full characterization of r84, a human IgG1 specific for VEGF-A, will be described in detail in a forthcoming manuscript.[4]

Reactivity of the antibodies to VEGF was analyzed by ELISA. VEGF (Sigma-Aldrich) at a concentration of 12.5 nmol/L (500 ng/mL) was coated directly on wells of a microtiter plate in the presence or absence of 0.81 pmol/L to 13 nmol/L (122–2,000 ng/mL) of control or test antibodies. The reactions were developed by the addition of peroxidase-labeled goat anti-mouse antibody (2C3) or anti-human antibody (r84, bevacizumab, XTL; Jackson Immunoresearch) and visualized by the addition of 3,3′5,5′-tetramethylbenzidine substrate (Kirkegaard and Perry Laboratories, Inc.). Reactions were stopped after 15 min with 10% HCl and read spectrophotometrically at 450 nm.

Tumor Model and Treatment
Six- to eight-week-old non-obese diabetic (NOD)/SCID mice were purchased from an on-campus supplier. Animals were housed in a pathogen-free facility, and all animal studies were done on a protocol approved by the Institutional Animal Care and Use Committee at the University of Texas Southwestern Medical Center. MDA-MB-231 cells (5×10^6) were injected into the mammary fat pad using previously described techniques (14, 15). Briefly, a small incision was made over the right axillary fat pad and the cells were injected in a volume of 50 μL using a 30-gauge needle. The incision was closed with a simple suture. Caliper measurements were done twice weekly, and tumor volume was calculated as $D \times d^2 \times 0.52$, wherein D is the long diameter and d is the perpendicular short diameter. Therapy was initiated on day 26 post tumor cell injection, when tumor volume reached ~150 mm^3. Animals were randomized to receive s.c. injection of saline control, 2C3, r84, or bevacizumab (250 μg of the designated IgG) twice weekly (Tuesday and Friday).

Immunohistochemistry
Tissue was snap frozen in liquid nitrogen, embedded in ornithine carbamyl transferase medium, and sectioned. Sections were fixed in acetone, briefly air dried, and blocked with 20% Aquablock (East Coast Biologics) for 30 to 60 min. Primary antibodies were used at a final concentration of 5 to 10 μg/mL; rat anti–mouse endothelial cell (MECA-32; Developmental Studies Hybridoma Bank, University of Iowa),

rat anti-CD31 (MEC13.3, BD Biosciences), rabbit anti–α-smooth muscle actin (RP-9010, NeoMarkers), rabbit anti-NG2 (AB5320, Millipore), mouse anti-VEGF (Gv39M; purified in our laboratory; ref. 32), goat anti-F4/80 (sc-26642, Santa Cruz Biotechnology), rat anti-Mac3 (Pharmingen), rat anti-CD16 (ebioscience), rat antineutrophil, 7/4 (MCA 7716, AbD Serotec), rat anti-CD83 (Michel-19, BioLegend), and rat anti-CD11b (M1/70, American Type Culture Collection); and purified in our laboratory. Primarily conjugated antibodies include phycoerythrin (PE)-labeled Gr1 (RB6-8C5), FITC-labeled CD11b (M1/70), and Alexa Fluor 488–labeled CD11c (N418) from Biolegend. Primary antibody was incubated on sections for 1 h at room temperature or overnight at 4°C. Negative controls were done by omitting the primary antibody. Following washes, the appropriate fluorophore-conjugated secondary antibody was added (Jackson Immunoresearch). Fluorescent slides were covered with coverslips using Prolong with 4′,6-diamidino-2-phenylindole (Invitrogen). Sections were examined on a Nikon E600 microscope, and images were captured with Photometrics Coolsnap HQ camera using Elements Software.

PCR

RNA was prepared using TRIzol (Invitrogen) according to the manufacturer's instructions. The quality of RNA was evaluated using spectrophotometry. The cDNA used for subsequent for PCR was made using iScript (Bio-Rad Laboratories) and Choice DNA Taq polymerase (Denville Scientific) was used for subsequent PCRs. The expression of *VEGFR2* (Hs00176676_m1), *VEGFR1* (Hs00176573_m1), *Nrp-1* (Hs1546494_m1), and *Nrp-2* (Hs00187290_m1) was analyzed by quantitative real-time reverse transcription-PCR (qRT-PCR) using an assay on demand (Mm00440111_m1) from Applied Biosystems. *GAPDH* (Applied Biosystems assay-on-demand) was used as an internal reference gene to normalize input cDNA. qRT-PCR was done in a reaction volume of 20 μL, including 1 μL of cDNA, and each reaction was done in triplicate. We used the comparative cycle threshold method to compute relative expression values (33). RNA isolated from human dermal microvascular endothelial cells was used a positive control for human VEGFR expression. RNA isolated from murine endothelial (bEnd.3) cells was used a negative control to show species specificity.

Isolation of Peritoneal Macrophages

Peritoneal macrophages were collected 6 wk after tumor cell injection by washing the peritoneal cavity with ice-cold RPMI medium with penicillin/streptomycin (pen/strep) (10 mL × 2 washes) and collecting the lavage fluid. The lavage fluid from tumor-bearing (*n* = 3) and non–tumor-bearing (*n* = 3) animals was pooled and centrifuged at 1,000 rpm for 5 min. The cells were plated overnight and washed with PBS the following morning. This procedure yielded cells that were >95% positive for the macrophage marker F4/80. These cells were used for immunocytochemistry and transwell migration assays.

Migration Assays

Migration assays were done using 24-well plates with either 3 μm (peritoneal macrophages) or 8 μm (MDA-MB-231) transwell inserts (Becton Dickinson Labware). Peritoneal macrophages (40,000) or MDA-MB-231 cells (20,000) in serum-free media were loaded onto the top of gelatin-coated or Matrigel-coated (BD Biosciences) filters. Forty nanograms of VEGF (R&D) in the presence or absence of the indicated IgG at 40 μg/mL were added to the lower chamber, and the cells were allowed to migrate overnight. The inserts were fixed and stained using Diff-Quick (VWR International). The number of cells per field (total magnification, ×400 macrophages or ×100 MDA-MB-231 cells) was counted manually. Each experiment was done in triplicate, and four to five fields per insert were counted.

Immunocytochemistry

Peritoneal macrophages were plated on chamber slides and maintained overnight at 37°C in a mixture of 5% CO_2 and 95% air in DMEM supplemented with 10% FCS. Cells were fixed in acetone and blocked with 20% Aquablock for 30 to 60 min. Primary antibodies were used at 5 μg/mL and included T014 (rabbit anti-VEGFR2 purified in our laboratory; ref. 34) and 9G10 (rat anti-VEGFR2 purified in our laboratory; ref. 35). The slides were developed with fluorophore conjugated secondary antibody, as described above.

Flow Cytometry

Tumor lysates were prepared by mincing the tumor in RPMI media (Sigma), incubating in collagenase for 1 h (Sigma), and filtering through sequentially smaller filters (BD Biosciences). The single-cell suspension was labeled with primary antibody for 30 min at 4°C. Antibodies specific for CD11b (M1/70-FITC, Biolegend) and VEGFR2 (89B3A5-PE, Biolegend) were used. Flow cytometry was done on FACSCaliber (BD Biosciences). Propidium iodide (Sigma) positive cells were excluded, and gates were adjusted on the negative control. These gates were then applied to tumor lysates. Data analysis was done using FloJo software (Tree Star, Inc.).

ELISA

Tumor lysates were made from orthotopic tumors by mincing the tumor in lysis buffer. Protein content was assayed using BCA assay (Pierce), and 100 μg of total protein were used in each assay. Human placental growth factor (PlGF) and VEGFR1 and mouse VEGF, PlGF, VEGFR1, and VEGFR2 Quantikine Immunoassays were done according to manufacturer's instructions (R&D Systems).

Proliferation Assay

MDA-MB-231 cells were seeded at 2,500 cells per well in a 96-well tissue culture plate. The cells were serum-starved for 24 h and subsequently stimulated with a medium containing 2% serum or VEGF at 50 ng/mL in the presence or absence of 2C3, bevacizumab, r84, or a control IgG, each at 95 μg/mL (500-fold molar excess VEGF). After incubating for 72 h, cell number was estimated by CellTiterGlo assay (Promega) according to the manufacturer's instructions.

Statistics

Data were analyzed using GraphPad software (GraphPad Prism version 4.00 for Windows, GraphPad Software[5]). Results are expressed as mean ± SEM. Data were analyzed

---

[5] http://www.graphpad.com

by *t* test or ANOVA, and results are considered significant at $P < 0.05$.

Results

r84 Inhibits Orthotopic Breast Tumor Growth

Inhibition of VEGF binding to VEGFR2 with 2C3 has been shown to reduce tumor size in pancreatic tumors (16, 17, 36) and breast tumors (14). We tested whether r84, a fully human antibody that inhibits VEGF binding to VEGFR2, would inhibit tumor growth in an orthotopic breast cancer model, similar to 2C3. Figure 1A shows the binding curves of r84, 2C3, and bevacizumab to human VEGF that display half-maximal binding of 0.014, 0.45, and 0.003 nmol/L, respectively. In an orthotopic human breast cancer xenograft model, chronic treatment with r84, 2C3, or bevacizumab significantly reduced ($P < 0.001$; days 44 and 48 versus control) the growth of established MDA-MB-231 tumors, such that there was a 55%, 62%, and 58% decrease,

Figure 1. r84 inhibits MDA-MB-231 tumor growth. **A,** wells were coated with human VEGF (Sigma-Aldrich) and were then incubated in the presence of the indicated IgG from 0.81 pmol/L to 13 nmol/L (0.122–2,000 ng/mL). The plate was developed using a peroxidase-conjugated goat anti-mouse antibody (2C3) or anti-human antibody (bevacizumab, r84, or XTL). Assays were done in triplicate. **B,** MDA-MB-231 human breast cancer cells (5×10^6) were injected into the mammary fat pad of SCID mice. Treatment with saline control ($n = 5$) or 250 μg of bevacizumab ($n = 8$), 2C3 ($n = 5$), or r84 ($n = 9$) was initiated in established tumors (150 mm^3) on day 26 post tumor cell injection (*TCI*) and continued for 3 wk. Tumor volumes were measured twice weekly. *Points,* mean tumor volume; *bars,* SE. Bevacizumab, r84, and 2C3 inhibited tumor growth compared with control. ∗∗∗, $P < 0.0001$, treatment versus control. Final tumor volume: control, 822.5 ± 160.1; 2C3, 309 ± 68.6; bevacizumab, 344 ± 29.4; r84, 368 ± 28.4 mm^3.

respectively, in tumor volume compared with control-treated animals (Fig. 1B). 2C3 and bevacizumab bind to human VEGF only; thus, these results show that inhibition of tumor cell–derived VEGF is sufficient for control of MDA-MB-231 tumors.

To determine if the effect of r84, 2C3, and bevacizumab on MDA-MB-231 tumor growth *in vivo* could be due to blocking VEGF activation of tumor cells directly, we evaluated tumor cell proliferation and migration *in vitro*. MDA-MB-231 *in vitro* proliferation was unaffected by VEGF, 2C3, bevacizumab, or r84 treatment (data not shown). However, we found that MDA-MB-231 cells migrated strongly toward VEGF, and this migration was blocked by the addition of 2C3, r84, or bevacizumab (Fig. 2A). These results suggest that VEGF binding to VEGFR2 and perhaps VEGFR1, expressed by MDA-MB-231 cells, induces cell migration.

The expression of VEGFR2 on MDA-MB-231 breast cancer cells has been controversial. Some groups have shown that minimal VEGFR2 is expressed on the cell surface (4), whereas others have shown that it is expressed at high levels following serum starvation (37). To examine VEGF receptor expression in MDA-MB-231 cells and tumors, we did qRT-PCR for VEGF receptors on whole cell lysates from MDA-MB-231 cells and tumors. Human dermal microvascular endothelial cells and murine (bEnd.3) endothelial cells were used as positive and negative controls, respectively, for testing the species specificity of the primers. We found that MDA-MB-231 cells expressed a detectable level of *VEGFR1, VEGFR2, NRP-1,* and *NRP-2 in vitro* (Fig. 2B). The expression of each receptor *in vivo* was compared with the level of expression *in vitro*. We found a 2.7-, 3.7-, and 8-fold increase in expression of *VEGFR1* in control, bevacizumab, and r84-treated tumors, respectively, compared with MDA-MD-231 cells *in vitro*. In contrast, the level of *VEGFR2* message did not change *in vivo* in any of the treatment groups. The level of *NRP-1* was elevated slightly (1.8- to 2.5-fold) *in vivo*, whereas *NRP-2* levels increased 6.9-, 7.9-, and 9.3-fold in tumors from mice treated with control, r84, and bevacizumab, respectively (Fig. 2C). These results show that *in vitro*, MDA-MB-231 cells express all VEGF receptors; however, levels of *VEGFR1, NRP-1,* and *NRP-2* are elevated when MDA-MB-231 cells are grown *in vivo*.

Next, we investigated the expression of VEGF-related proteins in serum and tumor lysates following treatment with control, 2C3, r84, and bevacizumab (Table 1). The only serum analytes that were altered significantly included mouse VEGF, human PlGF, and soluble mouse VEGFR1. Immunodepletion with protein G beads removed all detectable mouse VEGF from the serum of mice treated with r84. This is similar to Loupakis et al. (38), who found that serum levels of VEGF in cancer patients treated with bevacizumab were reduced significantly after immunodepletion. In addition, the serum level of soluble mouse VEGFR1 was elevated significantly ($P < 0.01$) by treatment with bevacizumab but not r84 or 2C3. In tumor lysates, we found significant treatment-induced changes in human PlGF and soluble mouse VEGFR1 (sVEGFR1). There was a significant decrease ($P < 0.001$) in the level of human PlGF in tumors from bevacizumab-treated animals compared with control,
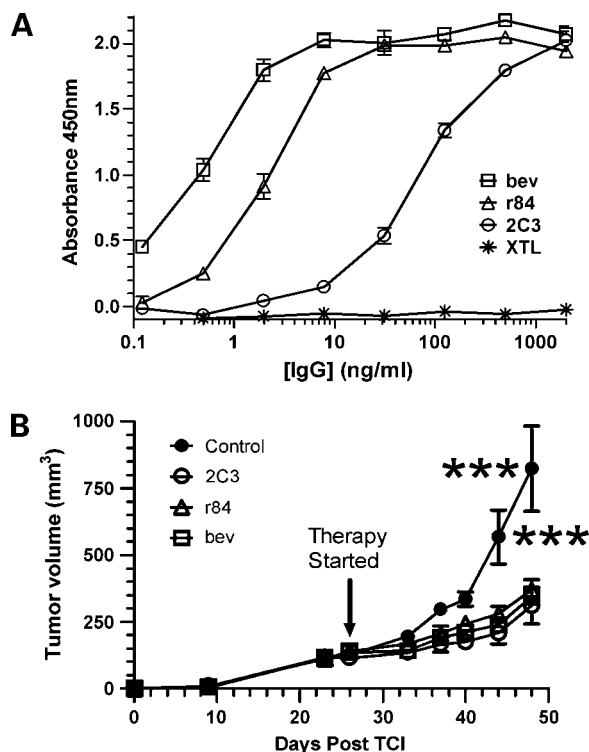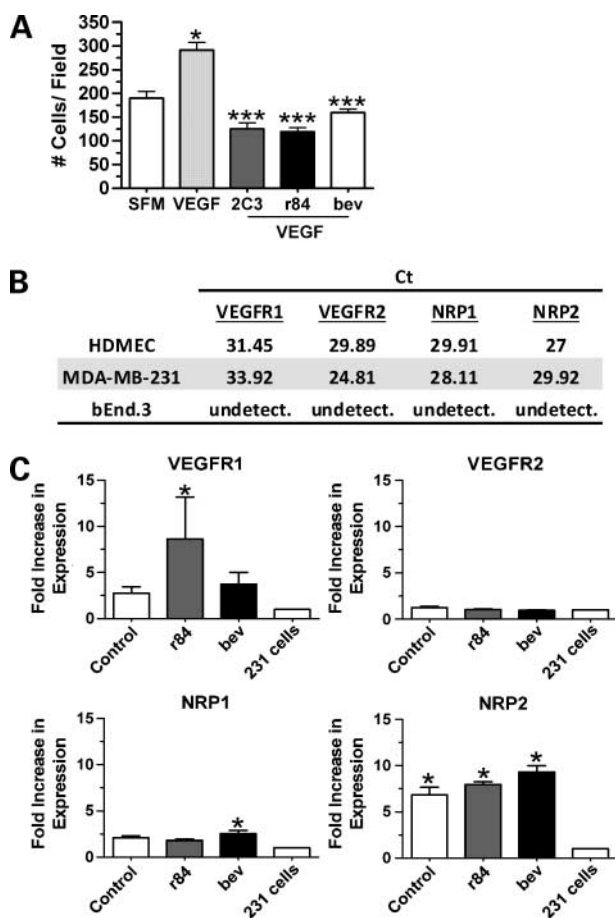
Figure 2. MDA-MB-231 cells express VEGF receptors, and VEGFR2 mediates tumor cell migration. **A,** *in vitro* migration assays were done using 24-well plates with 8-μm transwell inserts. MDA-MB-231 cells were allowed to migrate overnight toward serum-free medium, VEGF (40 ng/mL), or VEGF plus the indicated IgG (40 μg/mL). MDA-MB-231 migrated significantly toward VEGF (VEGF versus serum-free medium). *, $P < 0.05$. Migration was reduced in the presence of r84, 2C3, and bevacizumab. The mean number of cells per high-power field in each condition is shown. Six high-power fields were counted per insert. Assays were done in triplicate. * * *, $P < 0.001$, anti-VEGF treatment versus VEGF. **B,** RNA isolated from human dermal microvascular endothelial cells and murine (*bEnd.3*) endothelial cells and MDA-MB-231 cells was used for qRT-PCR analysis of *VEGFR1*, *VEGFR2*, *NRP-1*, and *NRP-2*. The mean cycle threshold value for each target is displayed. **C,** RNA was isolated from tumors at the time of sacrifice from control, bevacizumab-, and r84-treated animal and used for qRT-PCR. MDA-MB-231 cells express *VEGFR1*, *VEGFR2*, *NRP-1*, and *NRP-2*. The ratio of tumor cell expression *in vivo*/MDA-MB-231 cells *in vitro* is expressed as the fold increase in expression based on cycle threshold. Data are normalized to *GAPDH*. *, $P < 0.05$ versus MDA-MB-231 cells *in vitro*.

2C3-, or r84-treated animals. In addition, there was a significant decrease ($P < 0.001$) in mouse soluble VEGFR1 in tumors from all anti-VEGF therapies compared with control.

r84 Reduces VEGF-Induced Angiogenesis

Anti-VEGF therapy with 2C3, r84, or bevacizumab reduced tumor microvessel density by 50%, 45%, and 58%, respectively, as measured by immunohistochemistry with MECA-32 (Fig. 3A) and anti-CD31 (data not shown). In addition, we used the monoclonal antibody GV39M (32) to

evaluate the number of VEGF-activated blood vessels in tumors from control and anti-VEGF–treated animals. r84- or bevacizumab-treated tumors showed a marked decrease in GV39M staining (68% and 55%, respectively) compared with control-treated tumors, although this was only statistically significant in the r84-treated group (Fig. 3B). Tumors from 2C3-treated animals were not evaluated because of secondary antibody cross-reactivity with 2C3, which localizes to tumor stroma (32). Treatment with 2C3, r84, or bevacizumab also resulted in an increase in the percentage of endothelial cells associated with pericytes, as determined by colocalization of MECA-32 with α-smooth muscle actin (α-SMA; Fig. 3C) and CD31 with NG2 (Fig. 3C). These results are consistent with a "pruning" effect of anti-VEGF therapy on vessels not associated with support cells.

r84 Decreases Macrophage Infiltration into Breast Tumor Xenografts

Next, we evaluated macrophage infiltration into breast tumors from all treatment groups using three different macrophage markers. Immunofluorescence staining of tumor sections revealed that anti-VEGF therapy with 2C3, r84, and bevacizumab reduced the infiltration of F4/80^{+} (Fig. 4A), CD16^{+} (Fig. 4B), and Mac-3^{+} (Fig. 4C) cells into breast tumors. The reduction of macrophage infiltration in the face of treatment with 2C3 and r84 is presumably due to expression of VEGFR2 on tumor-associated macrophages (16).

To evaluate VEGFR2 expression on systemic macrophages, we harvested peritoneal macrophages from tumor-bearing and non–tumor-bearing animals and evaluated VEGFR2 expression by immunocytochemistry (Fig. 4D). Using two different anti-VEGFR2 antibodies, we show that peritoneal macrophages from tumor-bearing animals express significantly higher levels of VEGFR2 compared with peritoneal macrophages from non–tumor-bearing animals. VEGFR1 expression showed a similar expression pattern, whereby *VEGFR1* mRNA was undetectable in non–tumor-bearing animals but was detectable in peritoneal macrophages from tumor-bearing animals by RT-PCR (data not shown). To assess the functional significance of VEGFR2 expression on peritoneal macrophages, we analyzed VEGF-induced migration of peritoneal macrophages *ex vivo*. Peritoneal macrophages from non–tumor-bearing animals (VEGFR2^{-}) show only minimal migration toward VEGF, which is unaffected by the presence of 2C3 or control antibody, whereas peritoneal macrophages harvested from tumor-bearing animals (VEGFR2^{+}) migrate strongly toward VEGF, and this is abrogated by the addition of 2C3 (Fig. 4E).

Compensatory Increase in Neutrophil and Dendritic Cell Infiltration and Decrease in Myeloid-Derived Suppressor Cell Infiltration in Tumors from r84-Treated Animals

Previous studies have shown a role for VEGF in the splenic infiltration of myeloid-derived suppressor cells and dendritic cells (31). To determine if anti-VEGF therapy with r84, 2C3, or bevacizumab affects the infiltration of these immune cells into tumors, we characterized the number of 7/4^{+}, CD83^{+}/CD11c^{+}, CD11b^{+}/Gr1^{+}, and CD11b^{+}/VEGFR2^{+} cells in tumors

from each treatment group. In Fig. 5A, we show an increase in 7/4^{+} cells in tumors from mice treated with anti-VEGF antibodies, although this only reached statistical significance in the 2C3- and r84-treated groups. We also found an increase in CD83^{+}/CD11c^{+} dendritic cells (Fig. 5B) in tumors from mice treated with r84 compared with bevacizumab. However, when we evaluated the infiltration of cells expressing CD11b and Gr1 (Fig. 5C), we saw a 70% decrease ($P < 0.01$ versus control) in double-positive cells in tumors from mice treated with r84. Interestingly, 2C3 or bevacizumab treatment did not reduce the number of double-positive cells in the tumor. These results suggest a potential difference between inhibition of tumor- and host-derived VEGF-induced activation of VEGFR2 on recruitment of immune cells. We also evaluated the level of VEGFR2^{+} immune cells by flow cytometry. To show the presence of VEGFR2^{+} cells in tumors, we did three-color flow cytometry for CD11b and VEGFR2 on single-cell suspensions from two control and two r84-treated tumors. The two control tumors had 0.42% and 0.77% cells that were double positive, whereas the r84-treated tumors displayed 0.15% and 0.18% cells that expressed CD11b and VEGFR2 (Fig. 5D).

Discussion

The major findings of this study are that 2C3, r84, and bevacizumab effectively decrease tumor size, microvessel density, and macrophage infiltration in an orthotopic model of breast cancer. These data are consistent with previous findings (14–16, 25) and support the concept that reducing macrophage infiltration is an important aspect of anti-VEGF therapy. In addition, our study shows changes in other immune cell infiltrates (myeloid-derived suppressor cells, dendritic cells, and neutrophils), following anti-VEGF therapy.

Infiltrating inflammatory cells constitute a large component of the overall tumor mass (18, 19). VEGF is an abundant cytokine in the tumor microenvironment and is known to stimulate immune cell chemotaxis; however, few studies have looked directly at the effect of inhibitors of VEGF on immune cell infiltration into tumors. We have shown previously that 2C3 inhibits macrophage infiltration in an orthotopic pancreatic cancer model (16). In a mouse model of thyroid cancer, Salnikov et al. (25) showed that treatment with bevacizumab reduced macrophage infiltration. To our knowledge, this is the first report to show the effect of anti-VEGF therapy on neutrophil infiltration. Shojaei et al. (29) found that the number of CD11b^{+}Gr1^{+} cells increases following anti-VEGF therapy with bevacizumab in therapy refractive tumors but remains unchanged in therapy sensitive tumors, which is consistent with our results.

The innate immune system contributes to tumor progression through many different mechanisms, including (*a*) induction of DNA damage through the production of free radicals; (*b*) production of proangiogenic growth factors, cytokines, chemokines, and matrix metalloproteases; and (*c*) suppression of the adaptive immune response (18). The production of proinflammatory cytokines and growth factors is often argued as the primary mechanism through which the innate immune system contributes to tumor progression. Some of the important mediators include tumor necrosis factor α, transforming growth factor β, VEGF, interleukin 1β, and interleukin 6.

Because the production of cytokines and growth factors is one important mechanism by which immune cells contribute to tumor progression, we investigated the expression of many VEGF-related proteins by ELISA. We found that inhibition of VEGF signaling through VEGFR1 and VEGFR2 reduces significantly the amount of PlGF in tumor lysates, whereas selective inhibition of VEGF activation of VEGFR2 with 2C3 or r84 did not have this effect. Endothelial cell production of PlGF is regulated in part by VEGF, whereby PlGF expression is stimulated by VEGF in a dose-dependent manner (39). Given that the levels of PlGF were unchanged

Table 1. Comparison of cytokine and soluble receptor levels in animals treated with anti-VEGF therapy

	Control		Bevacizumab		r84		2C3	
	Tumor*	Serum[†]	Tumor	Serum	Tumor	Serum	Tumor	Serum
Ms VEGF	43.4 (3.3), n = 6	22.88 (7.0), n = 8	45.1 (1.8), n = 2	20.24 (5.4), n = 6	42.1 (3.3), n = 3	ND, n = 3	47.1 (3.9), n = 5	44.81 (13.6), n = 8
Hu PlGF	49.9 (2.7), n = 4	32.78 (6.0), n = 3	**2.4 (0.5),** n = 2[‡]	30.91 (8.7), n = 3	42.6 (1.9), n = 4	33.92 (6.2), n = 3	44.9 (11.0), n = 3	26.53 (3.6), n = 3
Ms PlGF	49.1 (3.8), n = 3	52.72 (15.8), n = 3	43.7 (12.9), n = 3	17 (4.7), n = 4	75.2 (4.6), n = 3	32.02 (12.1), n = 3	43.2 (8.1), n = 4	34.02 (9.5), n = 3
Hu sVEGFR1	1.9 (1.2), n = 4	ND; n = 4	ND, n = 2	ND, n = 3	0.5 (0.8), n = 4	ND, n = 3	1.5 (1.0), n = 5	ND, n = 5
Ms sVEGFR1	734.6 (49.9), n = 3	480.9 (68.2), n = 3	**394.8 (5.5),** **n = 2**	**906.4 (15.9),** **n= 2**	**479 (36.5),** **n = 4**	429.2 (52.3), n = 3	**344.2 (28.9),** **n = 3**	568.7 (76.1), n = 3
Ms sVEGFR2		86.98 (2.6), n = 6		82.12 (2.6), n = 3		88.16 (0.5), n = 3		91.68 (3.0), n = 6

NOTE: Mean (SE) is displayed. *n* is the number of tumors from the indicated group assayed in triplicate.
Abbreviation: ND, not determined; MS, mouse; Hu, human.
*Picogram per 100 μg of tumor lysate.
[†]Picogram per milliliter of serum.
[‡]Values in bold are statistically significant compared with control; all $P < 0.01$ or $P < 0.001$ by one-way ANOVA and Bonferroni's multiple comparison test.

Figure 3. r84 reduces VEGF-induced angiogenesis. Frozen sections of tumors from mice treated with control, 2C3, r84, and bevacizumab were analyzed by immunohistochemistry for expression of vascular markers. **A,** tumor sections were analyzed by immunofluorescence using MECA-32, an endothelial cell marker. Tumors from all anti-VEGF treatment groups showed a significant reduction in the number of vessels compared with control-treated tumors (control, 18.27 ± 2.2; 2C3, 9.13 ± 1.76; r84, 10.0 ± 1.57; bevacizumab, 7.73 ± 1.89 vessels per high-power field). *, $P < 0.05$; **, $P < 0.01$; ***, $P < 0.001$ versus control. **B,** tumor sections were analyzed by immunofluorescence using GV39M, which binds VEGF bound to VEGF receptor. There was a significant decrease in the amount of GV39M reactivity in tumors from r84-treated animals compared with control. *, $P < 0.05$. Data displayed as percentage of control fluorescent area ± SEM and represents five images per tumor and three tumors per group. **C,** tumor sections were colocalized with CD31 (*green*), an endothelial cell marker and NG2 (*red*), a pericyte marker, or Meca-32 and α-SMA, a pericyte marker. There was an increase in the number of pericyte-associated blood vessels in tumors from animals treated with all anti-VEGF therapies compared with control. Percentage of pericyte-associated blood vessels is displayed as mean ± SE and represents five images per tumor and three tumors per group. *, $P < 0.05$; **, $P < 0.01$ versus control. Representative images of CD31/NG2 staining in tumors from control- and r84-treated animals (total magnification for each image displayed, ×200). Images were overlaid using Elements software.
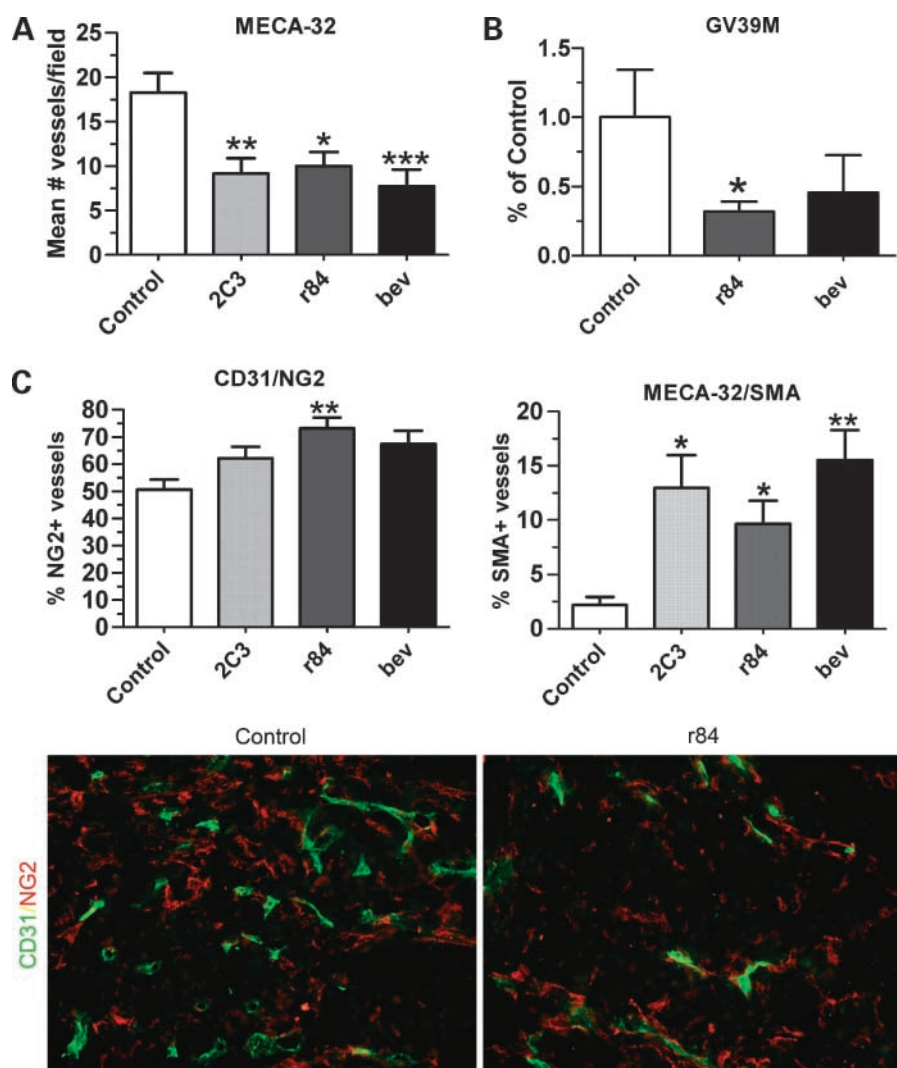
after treatment with r84 or 2C3, the decrease in PlGF levels in tumors treated with bevacizumab is likely due to decreased stimulation of VEGFR1 via VEGF. We also found that anti-VEGF therapy reduced the amount of soluble VEGFR1 (sVEGFR1) in the tumor. VEGFR1 transcription is regulated in part by VEGF activation of VEGFR1 and VEGFR2 (40) and oxygen levels, such that hypoxia stimulates sVEGFR1 expression (41). Furthermore, IFN-γ can also induce expression of sVEGFR1 (42). The decrease in sVEGFR1 levels after anti-VEGF therapy is likely due to reduced activation of VEGFR2 and/or changes in the cytokine profile of the tumors that results secondary to the change in immune cell infiltration.

2C3 and r84 selectively inhibit VEGF from interacting with VEGFR2 (13).[4] Therefore, for the decrease in macrophages to occur, we hypothesized that tumor-associated macrophages in this model express VEGFR2, as we have shown previously in an orthotopic model of pancreatic cancer (16). Furthermore, we show that peritoneal macrophages from tumor-bearing mice express VEGFR2, whereas peritoneal macrophages from non–tumor-bearing mice do not. *In vitro* migration studies further show that VEGFR2 is the dominant receptor responsible for the VEGF-dependent migration of these cells.

Although we saw a decrease in macrophage infiltration, we found an increase in neutrophil infiltration ($7/4^+$ cells) into tumors following treatment with each antibody. Neutrophils are often described as "first responders" and have been shown to be capable of mediating the angiogenic switch in engineered animal models of cancer (24, 26). The mechanism underlying the increase in $7/4^+$ cells after anti-VEGF therapy is unclear. VEGF has been shown to stimulate neutrophil migration *in vitro*. Interestingly, treatment with a neutralizing anti-VEGF antibody but not 2C3 abrogated VEGF-induced migration of neutrophils (43). Furthermore, these cells were shown to express *VEGFR1* and *VEGFR2* by RT-PCR, suggesting that although VEGFR2 is present, VEGFR1 is the primary receptor mediating VEGF-induced migration of these cells. An alternative explanation for the elevated neutrophil levels
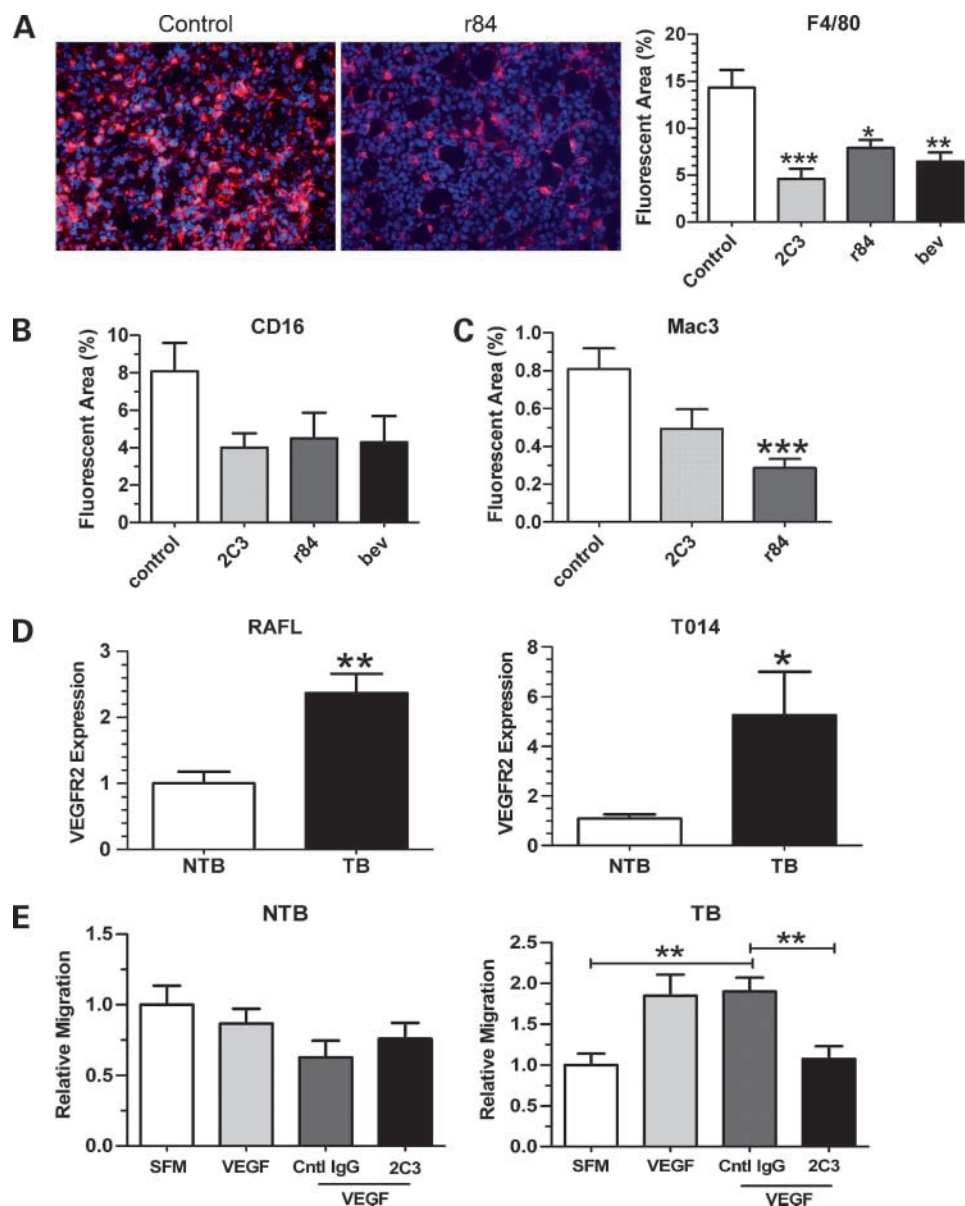
Mol Cancer Ther 2009;8(7). July 2009

Figure 4. r84 decreases macrophage infiltration into breast tumor xenografts. Frozen sections of tumors from mice treated with control, 2C3, r84, and bevacizumab were analyzed by immunohistochemistry for expression of macrophage markers. **A,** tumor sections from control, 2C3-, r84-, or bevacizumab-treated animals were evaluated by immunofluorescence with F4/80, a macrophage marker. Representative images of F4/80 staining in tumors from control and r84-treated animals (total magnification, ×200). There was a significant decrease in macrophage infiltration in tumors from all anti-VEGF groups compared with control-treated tumors. *, $P < 0.05$; **, $P < 0.01$; ***, $P < 0.001$. Data displayed are mean fluorescent area ± SE and represent three tumors per group, five high-power fields per slide. CD16+ (**B**) and Mac3+ (**C**) cells were also found to be reduced in tumors from anti-VEGF–treated animals compared with control. ***, $P < 0.001$. **D,** macrophages from tumor-bearing and non–tumor-bearing animals were isolated by peritoneal lavage, plated on chamber slides, and evaluated for VEGFR2 expression by immunocytochemistry using two different anti-VEGFR2 antibodies (*RAFL* and *T014*). Peritoneal macrophages from tumor-bearing animals have a significant increase in VEGFR2 expression compared with non–tumor-bearing animals. *, $P < 0.05$; **, $P < 0.01$. **E,** migration assays were done with primary peritoneal macrophages from non–tumor-bearing or tumor-bearing mice using 24-well plates with 3-μm transwell inserts. Peritoneal macrophages were allowed to migrate overnight toward serum-free medium, VEGF (40 ng/mL), or VEGF plus the indicated IgG (40 μg/mL). *Columns,* mean number of cells per high-power field in each condition; *bars,* SE. Four to five high-power fields were counted per insert. Assays were done in duplicate or triplicate. Data are displayed as fold change in migration compared with serum-free medium, are representative of at least three independent experiments, and were analyzed with Kruskal-Wallis test. VEGF and VEGF plus control IgG stimulated migration of macrophages from tumor-bearing animals compared with control. **, $P < 0.01$. This was abrogated by treatment with 2C3. **, $P < 0.01$.

is that the decrease of tumor-associated macrophages after anti-VEGF therapy results in reduced macrophage-mediated clearance of neutrophils that have degranulated (44, 45).

Defects in antigen presentation by dendritic cells is a mechanism by which tumors escape the host immune system. However, the causes of dendritic cell impairment are incompletely understood. VEGF is not only important

Figure 5. r84 modulates immune cell infiltration into breast tumor xenografts. Frozen sections of tumors from mice treated with control, 2C3, r84, and bevacizumab were analyzed by immunohistochemistry for expression of neutrophil (7/4) and mature dendritic cell (CD83/CD11c) markers. **A,** tumor sections from control 2C3, r84, or bevacizumab-treated animals were evaluated by immunofluorescence with 7/4, a granulocyte marker. Representative images of 7/4 staining in tumors from control- and r84-treated animals. Tumors from 2C3- and r84-treated animals showed a significant increase in 7/4$^+$ cells (*red*) compared with control-treated animals. *, $P < 0.05$. Nuclei were detected with 4′, 6-diamidino-2-phenylindole (*blue*). **B,** tumor sections were evaluated by immunofluorescence for mature dendritic cells. Representative images of tumor sections show colocalization (*yellow, white arrows*) of CD11c (*green*) and CD83 (*red*). Total magnification, ×200. The inset on each picture is a magnified view of colocalization. There was a significant increase in CD83$^+$ dendritic cells in r84-treated tumors but not in 2C3 or bevacizumab-treated tumors. *, $P < 0.05$. Quantification of immunofluorescence is based on five fields (×200) per tumor, at least three tumors per group. **C,** tumor sections were evaluated by immunofluorescence for myeloid-derived suppressor cells. Representative images of tumor sections show colocalization (*yellow*) of CD11b (*green*) and Gr1 (*red*). There was a significant decrease in CD11b$^+$Gr1$^+$ cells in r84-treated tumors but not in 2C3 or bevacizumab-treated tumors. **, $P < 0.01$. Images are representative from at least three tumors per group. Total magnification, ×200. Quantification of immunofluorescence is based on five fields (×200) per tumor. **D,** flow cytometry using anti–CD11b-FITC (*X axis*) and anti–VEGFR2-PE (*Y axis*) was done on single-cell suspensions made from control and r84-treated tumors and showed a population of VEGFR2+ macrophages in tumors from both groups (*top right quadrant*). There was a trend toward decreased VEGFR2+ macrophages in tumors from r84-treated animals compared with controls (0.77% and 0.42% for control versus 0.15% and 0.18% for r84). Data are two separate tumors from each group.
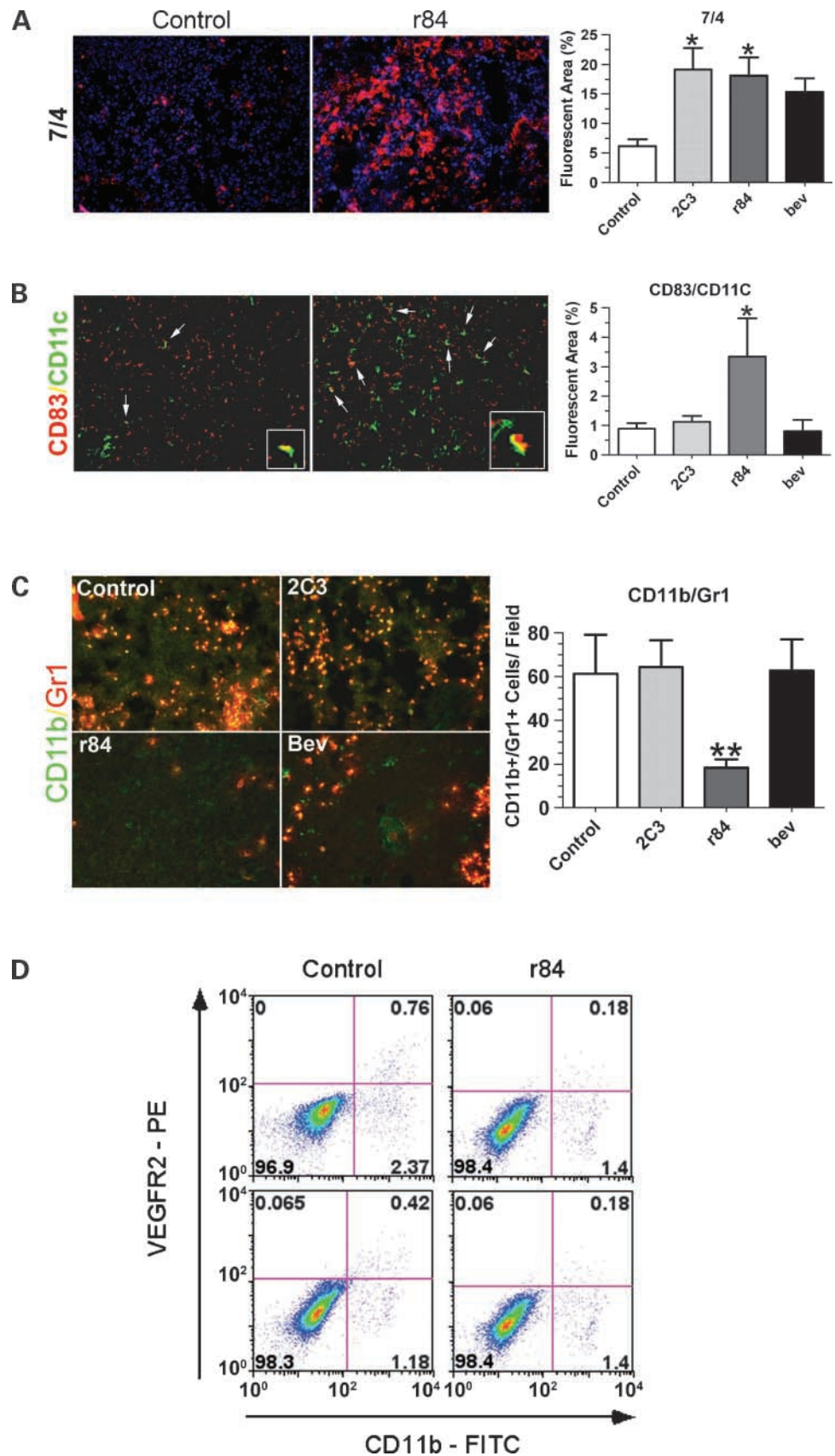
for monocyte chemotaxis but is a key regulator in the differentiation and migration of dendritic cells (31, 46). In the present study, we found an increase in the number of CD83$^+$CD11c$^+$ cells in tumors from r84-treated mice compared with bevacizumab-treated tumors. This finding could represent changes in either migration or differentiation of dendritic cells, given the differing roles of VEGFR1 and VEGFR2 in dendritic cell development. In non–tumor-bearing animals, VEGFR1 activation inhibits stem cell differentiation to the dendritic cell lineage, whereas VEGFR2 activation decreases the number and function of mature dendritic cells in the spleen (31). Our findings indicate that, in tumor-bearing animals, VEGFR2 activation is important for the infiltration of CD83$^+$ dendritic cells and that inhibition of VEGF binding to VEGFR2 via r84 leads to an increase in the infiltration of CD83$^+$CD11c$^+$ cells in breast tumor xenografts. Clinically, increased levels of CD83$^+$ cells correlates with decreased lymph node metastases in breast cancer patients, highlighting the importance of these cells in cancer immunity (30).

Interestingly, the number of CD11b$^+$Gr1$^+$ cells was reduced in tumors from mice treated with r84 but remained unchanged in tumors from 2C3- and bevacizumab-treated animals. Cells that express CD11b and Gr1 include myeloid-derived suppressor cells, which have been reported to affect response to anti-VEGF therapy (29). In the tumor microenvironment, these cells secrete immunosuppressive mediators and induce T-lymphocyte dysfunction (27, 28, 47). Other cell types besides myeloid-derived suppressor cells that are known to express CD11b and Gr1 include neutrophils and Tie-2–positive macrophages (48). Myeloid-derived suppressor cells have been reported to express VEGFR1 and VEGFR2 (48). Systemic treatment with VEGF induces myeloid-derived suppressor cell infiltration into the spleen compared with PBS control. Furthermore, blockade with anti-VEGFR2 abrogates this infiltration, suggesting a role of VEGFR2 in myeloid-derived suppressor cell infiltration into the spleen (31); however, the effect of VEGF on recruitment or activity of these cells into tumors is unclear. Our results suggest a differential effect of blocking VEGF activation of VEGFR1 and VEGFR2 versus blocking activation of VEGFR2 alone. VEGF activation of VEGFR1 in these cells might induce differentiation or block recruitment. Alternatively, selective activation of VEGFR1 might have a negative effect on VEGFR2 activity in these cells, as has been shown in endothelial cells in the eye after laser-induced injury (5). An area of interest is the cytokine milieu in tumors from mice treated with r84 or bevacizumab. If differences in the cytokine profile are found after treatment with these two agents, it could provide an explanation for the differential recruitment of CD11b$^+$Gr1$^+$ cells.

Although our study uses immunocompromised animals, the xenograft system used highlights the importance of tumor cell–derived factors with the use of human specific therapies (eg., 2C3, bevacizumab). However, the results should be interpreted with care (49) and future experiments have been designed to use immunocompetent animals. We anticipate that use of a mouse chimeric version of r84 will facilitate these studies and help solidify the function of VEGF in the recruitment of immune cells into solid tumors.

In summary, we have found that inhibition of VEGF-A with a fully human anti-VEGF antibody reduces VEGF-induced angiogenesis and breast tumor growth in mice. Furthermore, we have shown that blockade of VEGF signaling differentially affects the immune cell profile of breast tumor xenografts, which could have significant implications for the clinical use of current and future anti-VEGF therapies.

Disclosure of Potential Conflicts of Interest

Acknowledgments

References

1. Folkman J. Angiogenesis in cancer, vascular, rheumatoid and other disease. Nat Med 1995;1:27–31.

2. Pradeep CR, Sunila ES, Kuttan G. Expression of vascular endothelial growth factor (VEGF) and VEGF receptors in tumor angiogenesis and malignancies. Integr Cancer Ther 2005;4:315–21.

3. Yang AD, Camp ER, Fan F, et al. Vascular endothelial growth factor receptor-1 activation mediates epithelial to mesenchymal transition in human pancreatic carcinoma cells. Cancer Res 2006;66:46–51.

4. Lee TH, Seng S, Sekine M, et al. Vascular endothelial growth factor mediates intracrine survival in human breast carcinoma cells through internally expressed VEGFR1/FLT1. PLoS Med 2007;4:e186.

5. Nozaki M, Sakurai E, Raisler BJ, et al. Loss of SPARC-mediated VEGFR-1 suppression after injury reveals a novel antiangiogenic activity of VEGF-A. J Clin Invest 2006;116:422–9.

6. Autiero M, Waltenberger J, Communi D, et al. Role of PlGF in the intra- and intermolecular cross talk between the VEGF receptors Flt1 and Flk1. Nat Med 2003;9:936–43.

7. Ghosh S, Sullivan CA, Zerkowski MP, et al. High levels of vascular endothelial growth factor and its receptors (VEGFR-1, VEGFR-2, neuropilin-1) are associated with worse outcome in breast cancer. Hum Pathol 2008;39:1835–43.

8. Shraga-Heled N, Kessler O, Prahst C, Kroll J, Augustin H, Neufeld G. Neuropilin-1 and neuropilin-2 enhance VEGF121 stimulated signal transduction by the VEGFR-2 receptor. FASEB J 2007;21:915–26.

9. Hurwitz H, Fehrenbacher L, Novotny W, et al. Bevacizumab plus irinotecan, fluorouracil, and leucovorin for metastatic colorectal cancer. N Engl J Med 2004;350:2335–42.

10. Miller K, Wang M, Gralow J, et al. Paclitaxel plus bevacizumab versus paclitaxel alone for metastatic breast cancer. N Engl J Med 2007;357:2666–76.

11. Wilhelm SM, Adnane L, Newell P, Villanueva A, Llovet JM, Lynch M. Preclinical overview of sorafenib, a multikinase inhibitor that targets both Raf and VEGF and PDGF receptor tyrosine kinase signaling. Mol Cancer Ther 2008;7:3129–40.

12. Lacouture ME, Wu S, Robert C, et al. Evolving strategies for the management of hand-foot skin reaction associated with the multitargeted kinase inhibitors sorafenib and sunitinib. Oncologist 2008;13:1001–11.

13. Brekken RA, Overholser JP, Stastny VA, Waltenberger J, Minna JD, Thorpe PE. Selective inhibition of vascular endothelial growth factor (VEGF) receptor 2 (KDR/Flk-1) activity by a monoclonal anti-VEGF antibody blocks tumor growth in mice. Cancer Res 2000;60:5117–24.

14. Whitehurst B, Flister MJ, Bagaitkar J, et al. Anti-VEGF-A therapy reduces lymphatic vessel density and expression of VEGFR-3 in an orthotopic breast tumor model. Int J Cancer 2007;121:2181–91.

15. Zhang W, Ran S, Sambade M, Huang X, Thorpe PE. A monoclonal antibody that blocks VEGF binding to VEGFR2 (KDR/Flk-1) inhibits vascular expression of Flk-1 and tumor growth in an orthotopic human breast cancer model. Angiogenesis 2002;5:35–44.

16. Dineen SP, Lynn KD, Holloway SE, et al. Vascular endothelial growth factor receptor 2 mediates macrophage infiltration into orthotopic pancreatic tumors in mice. Cancer Res 2008;68:4340–6.

17. Holloway SE, Beck AW, Shivakumar L, Shih J, Fleming JB, Brekken RA. Selective blockade of vascular endothelial growth factor receptor 2 with an antibody against tumor-derived vascular endothelial growth factor controls the growth of human pancreatic adenocarcinoma xenografts. Ann Surg Oncol 2006;13:1145–55.

18. de Visser KE, Eichten A, Coussens LM. Paradoxical roles of the immune system during cancer development. Nat Rev Cancer 2006;6:24–37.

19. Coussens LM, Werb Z. Inflammation and cancer. Nature 2002;420:860–7.

20. Leek RD, Lewis CE, Whitehouse R, Greenall M, Clarke J, Harris AL. Association of macrophage infiltration with angiogenesis and prognosis in invasive breast carcinoma. Cancer Res 1996;56:4625–9.

21. Talmadge JE, Donkor M, Scholar E. Inflammatory cell infiltration of tumors: Jekyll or Hyde. Cancer Metastasis Rev 2007;26:373–400.

22. Lin EY, Pollard JW. Tumor-associated macrophages press the angiogenic switch in breast cancer. Cancer Res 2007;67:5064–6.

23. Zeisberger SM, Odermatt B, Marty C, Zehnder-Fjallman AH, Ballmer-Hofer K, Schwendener RA. Clodronate-liposome-mediated depletion of tumour-associated macrophages: a new and highly effective antiangiogenic therapy approach. Br J Cancer 2006;95:272–81.

24. Pahler JC, Tazzyman S, Erez N, et al. Plasticity in tumor-promoting inflammation: impairment of macrophage recruitment evokes a compensatory neutrophil response. Neoplasia 2008;10:329–40.

25. Salnikov AV, Heldin NE, Stuhr LB, et al. Inhibition of carcinoma cell-derived VEGF reduces inflammatory characteristics in xenograft carcinoma. Int J Cancer 2006;119:2795–802.

26. Nozawa H, Chiu C, Hanahan D. Infiltrating neutrophils mediate the initial angiogenic switch in a mouse model of multistage carcinogenesis. Proc Natl Acad Sci U S A 2006;103:12493–8.

27. Serafini P, De Santo C, Marigo I, et al. Derangement of immune responses by myeloid suppressor cells. Cancer Immunol Immunother 2004;53:64–72.

28. Gabrilovich DI, Velders MP, Sotomayor EM, Kast WM. Mechanism of immune dysfunction in cancer mediated by immature Gr-1 + myeloid cells. J Immunol 2001;166:5398–406.

29. Shojaei F, Wu X, Malik AK, et al. Tumor refractoriness to anti-VEGF treatment is mediated by CD11b + Gr1 + myeloid cells. Nat Biotechnol 2007;25:911–20.

30. Iwamoto M, Shinohara H, Miyamoto A, et al. Prognostic value of tumor-infiltrating dendritic cells expressing CD83 in human breast carcinomas. Int J Cancer 2003;104:92–7.

31. Huang Y, Chen X, Dikov MM, et al. Distinct roles of VEGFR-1 and VEGFR-2 in the aberrant hematopoiesis associated with elevated levels of VEGF. Blood 2007;110:624–31.

32. Brekken RA, Huang X, King SW, Thorpe PE. Vascular endothelial growth factor as a marker of tumor endothelium. Cancer Res 1998;58:1952–9.

33. Karlen Y, McNair A, Perseguers S, Mazza C, Mermod N. Statistical significance of quantitative PCR. BMC Bioinformatics 2007;8:1–16.

34. Feng D, Nagy JA, Brekken RA, et al. Ultrastructural localization of the vascular permeability factor/vascular endothelial growth factor (VPF/VEGF) receptor-2 (FLK-1, KDR) in normal mouse kidney and in the hyperpermeable vessels induced by VPF/VEGF-expressing tumors and adenoviral vectors. J Histochem Cytochem 2000;48:545–56.

35. Ran S, Huang X, Downes A, Thorpe PE. Evaluation of novel anti-mouse VEGFR2 antibodies as potential antiangiogenic or vascular targeting agents for tumor therapy. Neoplasia 2003;5:297–307.

36. Korpanty G, Carbon JG, Grayburn PA, Fleming JB, Brekken RA. Monitoring response to anticancer therapy by targeting microbubbles to tumor vasculature. Clin Cancer Res 2007;13:323–30.

37. Liang Y, Brekken RA, Hyder SM. Vascular endothelial growth factor induces proliferation of breast cancer cells and inhibits the anti-proliferative activity of anti-hormones. Endocr Relat Cancer 2006;13:905–19.

38. Loupakis F, Falcone A, Masi G, et al. Vascular endothelial growth factor levels in immunodepleted plasma of cancer patients as a possible pharmacodynamic marker for bevacizumab activity. J Clin Oncol 2007;25:1816–8.

39. Yao YG, Yang HS, Cao Z, Danielsson J, Duh EJ. Upregulation of placental growth factor by vascular endothelial growth factor via post-transcriptional mechanism. FEBS Lett 2005;579:1227–34.

40. Wang D, Donner DB, Warren RS. Homeostatic modulation of cell surface KDR and Flt1 expression and expression of the vascular endothelial cell growth factor (VEGF) receptor mRNAs by VEGF. J Biol Chem 2000;275:15905–11.

41. Munaut C, Lorquet S, Pequeux C, et al. Hypoxia is responsible for soluble vascular endothelial growth factor receptor-1 (VEGFR-1) but not for soluble endoglin induction in villous trophoblast. Hum Reprod 2008;23:1407–15.

42. Kommineni VK, Nagineni CN, William A, Detrick B, Hooks JJ. IFN-γ acts as anti-angiogenic cytokine in the human cornea by regulating the expression of VEGF-A and sVEGF-R1. Biochem Biophys Res Commun 2008;374:479–84.

43. Ancelin M, Chollet-Martin S, Herve MA, Legrand C, El Benna J, Perrot-Applanat M. Vascular endothelial growth factor VEGF189 induces human neutrophil chemotaxis in extravascular tissue via an autocrine amplification mechanism. Lab Invest 2004;84:502–12.

44. Michlewska S, Dransfield I, Megson IL, Rossi AG. Macrophage phagocytosis of apoptotic neutrophils is critically regulated by the opposing actions of pro-inflammatory and anti-inflammatory agents: key role for TNF-{α}. FASEB J 2008;23:844–54.

45. Noonan DM, De Lerma Barbaro A, Vannini N, Mortara L, Albini A. Inflammation, inflammatory cells and angiogenesis: decisions and indecisions. Cancer Metastasis Rev 2008;27:31–40.

46. Dikov MM, Ohm JE, Ray N, et al. Differential roles of vascular endothelial growth factor receptors 1 and 2 in dendritic cell differentiation. J Immunol 2005;174:215–22.

47. Talmadge JE. Pathways mediating the expansion and immunosuppressive activity of myeloid-derived suppressor cells and their relevance to cancer therapy. Clin Cancer Res 2007;13:5243–8.

48. Murdoch C, Muthana M, Coffelt SB, Lewis CE. The role of myeloid cells in the promotion of tumour angiogenesis. Nat Rev Cancer 2008;8:618–31.

49. Talmadge JE, Singh RK, Fidler IJ, Raz A. Murine models to evaluate novel and conventional therapeutic strategies for cancer. Am J Pathol 2007;170:793–804.